Am J Clin Exp Immunol 2025;14(4):223-236
www.ajcei.us /ISSN:2164-7712/AJCEI0164044

Original Article

DPT has potential to be a prognostic biomarker and its correlation with immune infiltrates in prostate cancer

Jieyu Jin[1], Junchao Feng[2], Tong Zhou[1,3], Jun Cao[1], Bin Feng[1], Qingqin Tang[1], Sheng Zhang[1], Jun Qiu[1], Yuting Liang[1]

[1]Center for Clinical Laboratory, The First Affiliated Hospital of Soochow University, Suzhou 215006, Jiangsu, China; [2]Department of Nuclear Accident Medical Emergency, The Second Affiliated Hospital of Soochow University, Suzhou 215004, Jiangsu, China; [3]Medical College of Soochow University, Suzhou 215123, Jiangsu, China

Received February 19, 2025; Accepted August 7, 2025; Epub August 15, 2025; Published August 30, 2025

Abstract: Background: Prostate cancer (PRAD) poses a significant threat to male health. The tumor microenvironment (TME) plays a crucial role in its development process, yet the regulatory significance of specific extracellular matrix proteins such as Dermatopontin (DPT) in PRAD remains poorly understood. Methods: A total of 534 PRAD transcriptome profiles were retrieved from The Cancer Genome Atlas (TCGA) database. CIBERSORT and ESTIMATE computational methods were used to quantify the presence of immune and stromal components. Differentially expressed genes (DEGs) were identified based on ImmuneScore and StromalScore, followed by Gene Ontology (GO) and Kyoto Encyclopedia of Genomes (KEGG) pathway enrichment analyses. DPT expression was analyzed in relation to overall survival, TNM staging, immune-related pathways using Gene Set Enrichment Analysis (GSEA), and tumor-infiltrating immune cells (TICs). Results: A total of 454 DEGs overlapping between high ImmuneScore and StromalScore groups were enriched in immune-related processes and pathways. DPT expression was positively correlated with the survival of PRAD patients, especially the N Stage of PRAD. GSEA revealed that high DPT expression correlated with immune-related activities such as allograft rejection, apical junction, complement, and epithelial mesenchymal transition while low DPT expression was correlated with metabolic pathways such as E2f targets, G2m checkpoint, mitotic spindle, and mitorc1 signaling. Analysis of TICs showed that DPT expression was positively correlated with resting mast cells and neutrophils. Conversely, regulatory T cells, M1 macrophages, M2 macrophages, and resting dendritic cells exhibited negative correlations with DPT expression. Conclusions: DPT may serve as a novel prognostic biomarker in PRAD, potentially affecting the survival of PRAD patients by regulating the immune environment of TME. These findings provide new insights into the immunomodulatory role of DPT and its potential as a therapeutic target for PRAD.

Keywords: DPT, tumor microenvironment, immune infiltration, prostate cancer

Introduction

Prostate cancer (PRAD) is one of the most prevalent malignancies among men worldwide and ranks as the second leading cause of cancer-related mortality, following lung cancer [1, 2]. Although many cases progress slowly, advanced PRAD can metastasize to the lymph nodes and bone, significantly compromising patient prognosis [3]. Despite progress in surgery, radiotherapy, and androgen deprivation therapy [4], treatment resistance and disease recurrence remain major clinical challenges. Consequently, the identification of reliable biomarkers for early detection, risk stratification, and immunotherapy prediction has become a priority in PRAD research.

Growing evidence suggests that tumor microenvironment (TME) - a complex milieu comprising immune cells, stromal components, extracellular matrix (ECM), and soluble factors, plays a central role in cancer progression and immune evasion [5-9]. Tumor-infiltrating immune cells (TICs), as key elements of TME, are known to influence therapeutic response and clinical outcome in PRAD [10-12]. Nevertheless, unlike other immunogenic tumors, PRAD exhibits a relatively immunosuppressive TME, often resulting in limited response to immune check-

point blockade therapies [13-15]. While several computational algorithms such as ESTIMATE and CIBERSORT have been used to quantify immune and stromal cell proportions in tumors, the immunoregulatory roles of specific TME-associated genes remain insufficiently characterized in PRAD.

Dermatopontin (DPT), a small extracellular matrix protein, has been implicated in cell adhesion, matrix remodeling, and immune regulation in various cancer types, including breast and liver cancers [16, 17]. However, its role in the immune landscape of PRAD is largely unexplored. In this study, we systematically analyzed transcriptomic data from the Cancer Genome Atlas (TCGA)-PRAD cohort to evaluate the prognostic value and immunological relevance of DPT. By integrating immune scoring, gene set enrichment analysis (GSEA), and immune cell deconvolution via CIBERSORT, we aimed to elucidate the correlation between DPT expression, TICs, and clinical outcomes. Our findings suggest that DPT may serve as a novel prognostic biomarker and a potential modulator of immune infiltration in TME of PRAD.

Materials and methods

Raw data acquisition

We obtained transcriptome RNA-seq data from TCGA database (https://portal.gdc.cancer.gov/) for our study on PRAD patients [18]. A total of 534 PRAD cases were included, consisting of 51 normal samples and 483 tumor samples. Additionally, corresponding clinical data such as stage, TNM classification, survival and outcome were also downloaded from TCGA database [19].

Analysis of ImmuneScore, StromalScore and ESTIMATEScore

Based on the gene expression data of the TCGA-PRAD cohort, the ESTIMATE algorithm was used to calculate the ImmuneScore, StromalScore and ESTIMATEScore to characterize TME of PRAD using R package estimate [20]. Higher scores in ImmuneScore or StromalScore indicate a greater abundance of immune or stromal components in TME, respectively. ESTIMATEScore, derived by summing ImmuneScore and StromalScore, represents the combined proportion of both components in TME.

Survival analysis

For survival analysis, we utilized R language with the survival and survminer packages. A total of 483 tumor samples had available records of detailed survival time, spanning from 0 to 13.8 years. To plot the survival curve, we employed the Kaplan-Meier method. Additionally, we used the log-rank test as the statistical significance test to evaluate the differences in survival outcomes.

DEGs between high-score and low-score groups

We categorized the 483 tumor samples into high-score or low-score groups based on the median score of ImmuneScore and StromalScore. Subsequently, limma package was used to identify differentially expressed genes (DEGs) between high-score and low-score groups. Specifically, the DEGs with fold changes greater than 1 and a false discovery rate (FDR) less than 0.05, following $\log_2$ transformation of the expression levels in the high and low score groups, were considered statistically significant. Additionally, heatmaps of the DEGs were generated using R package pheatmap to visualise the expression patterns of these genes across different samples.

GO and KEGG enrichment analysis

As previously described [21-23], Gene Ontology (GO) and Kyoto Encyclopedia of Genomes (KEGG) enrichment analysis were performed on 454 DEGs. These analysis were carried out in R with the assistance of packages such as clusterProfiler, enrichplot, and ggplot2 [24]. Significantly enriched terms were identified based on both *P*-value and *q*-value thresholds less than 0.05.

Difference analysis of clinical stages

The clinicopathological characteristics data corresponding to the PRAD samples were obtained from TCGA. The Wilcoxon rank sum test or the Kruskal-Wallis rank sum test was used to assess differences in different clinical stages of PRAD patients, providing valuable insights into the associations between clinical variables and molecular profiles.

Gene set enrichment analysis

We downloaded the Hallmark and C7 gene sets v6.2 collections from the Molecular Signatures

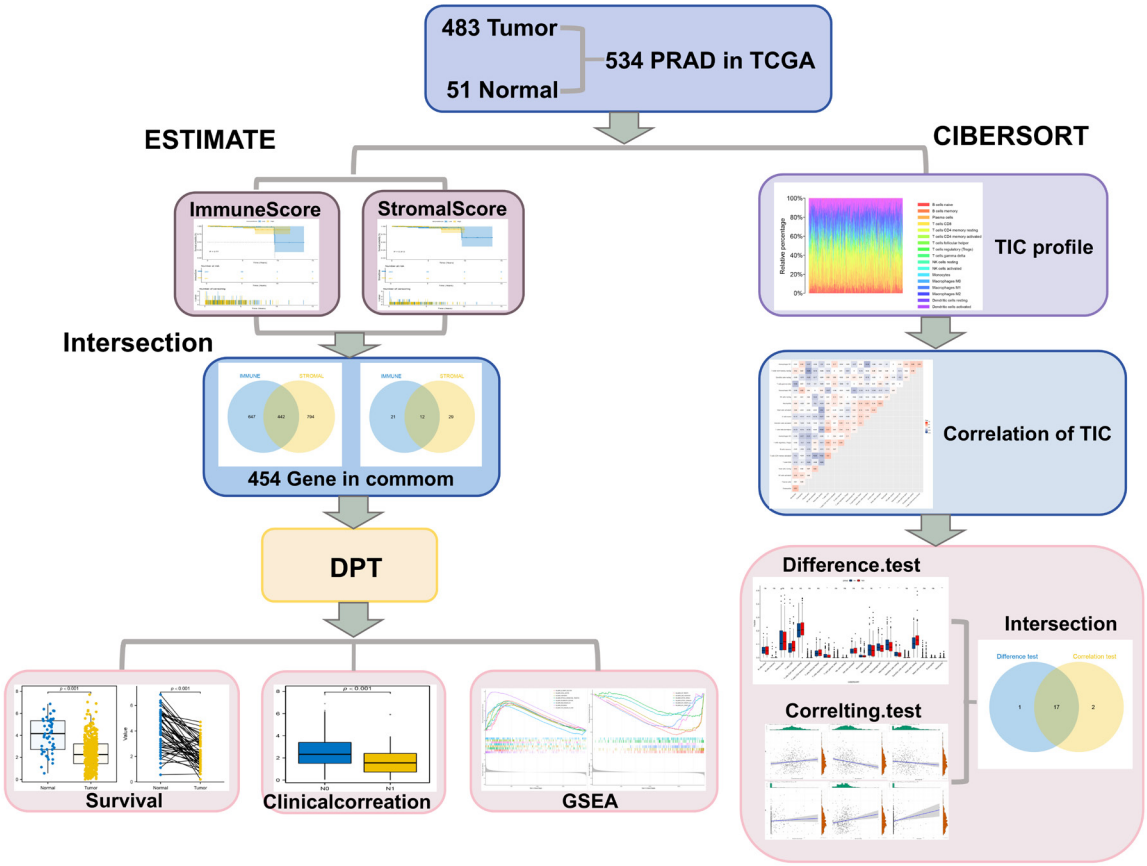

Figure 1. Analysis workflow of this study.

Database to serve as the target sets for GSEA as previously described [25, 26], GSEA enrichment analysis was performed using the R package clusterpofiler. GSVA scores were generated for all tumor samples based on transcriptomic data. Gene sets with a nominal *P*-value (NOM *P*-value) less than 0.05 and a FDR *q*-value less than 0.06 were considered statistically significant.

TICs profile

The CIBERSORT computational method was utilized to estimate the TICs abundance profile in all tumor samples. Subsequently, a quality filtering step was implemented, where only tumor samples with a *P*-value less than 0.05 were retained for further analysis. This rigorous selection criterion ensured that only samples with reliable estimations of immune cell abundance were included in the subsequent analysis, enhancing the robustness and accuracy of the findings related to the tumor immune microenvironment.

Statistical analysis

Wilcoxon test and one-way analysis of variance were used to compare the DPT expression level of PRAD in cancer tissue and normal tissue. For survival comparisons between high and low DPT expression, the Logrank test will be used. $P<0.05$ was considered statistically significant.

Results

Analysis process of this study

The analysis process of our study is shown in **Figure 1**. Firstly, we retrieved 534 transcriptome RNA-seq data from the TCGA database and processed them using the CIBERSORT and ESTIMATE algorithms to calculate Immune and Stromal scores. Subsequently, we utilized the Gene profile analysis and functional enrichment analysis in PRAD samples. Lastly, our focus shifted towards survival analysis, clinicopathological correlation analysis, Cox regres-

sion, GSEA and correlation with TICs specifically for DPT.

Analysis of ImmuneScore, StromalScore and ESTIMATEScore

All PRAD samples were divided into high and low score groups based on the median of each score (ImmuneScore, StromalScore, EstimatScore). To assess the correlation between the proportions of Immune and Stromal components and survival outcomes, Kaplan-Meier survival analysis was conducted on ImmuneScore, StromalScore, and ESTIMATEScore. As shown in **Figure 2A-C**, ImmuneScore, StromalScore and ESTIMATEScore did not exhibit significant correlations with overall survival rate.

Gene profile analysis and functional enrichment analysis

As shown in **Figure 3A**, **3B**, we found that compared to the median, ImmuneScore displayed 1122 DEGs in both high and low scoring samples. Among them, 1089 genes were upregulated and 33 genes were downregulated. Similarly, StromalScore analysis generated 1277 DEGs, of which 1236 genes were upregulated and 41 genes were downregulated (**Figure 3A**, **3B**). The Venn plot intersection analysis showed that 442 identical genes were up-regulated in the ImmuneScore and StromalScore groups, while 12 identical genes were down-regulated. Furthermore, GO enrichment analysis highlighted that the DEGs predominantly mapped to immune-related GO terms, encompassing functions such as leukocyte cell-cell adhesion, leukocyte proliferation, lymphocyte proliferation, mononuclear cell proliferation, and regulation of T cell activation (**Figure 3C**). Additionally, KEGG enrichment analysis underscored the enrichment of pathways including cell adhesion molecules, cytokine-cytokine receptor interaction, hematopoietic cell lineage, intestinal immune network for IgA production, and viral protein interaction with cytokine and cytokine receptor (**Figure 3D**).

The correlation of DPT expression with the survival and TNM stages

Survival analysis showed that PRAD patients with high DPT expression had longer overall survival than did PRAD patients with low DPT expression (**Figure 4C**). Furthermore, the Wilcoxon rank sum test demonstrated that the expression of DPT in tumor samples was significantly lower than that in normal samples (**Figure 4A**). Similar results were observed in the paired analysis between normal and tumor tissues from the same patient (**Figure 4B**). In addition, there was a significant correlation between DPT expression and the N Stage of PRAD (**Figure 4D**).

GSEA enrichment analysis

Figure 5A indicated that genes in the DPT high-expression group are primarily enriched in immune-related activities, such as allograft rejection, apical junction, complement, and epithelial mesenchymal transition. Conversely, genes in the DPT low-expression group are enriched in E2f targets, G2m checkpoint, mitotic spindle, and mitorc1 signaling, as depicted in **Figure 5B**. Additionally, when considering the C7 collection defined by MSigDB, immune-related gene sets were found to be enriched in the high DPT expression group, including macrophage, B cell, and $CD4^+$ T cell pathways (**Figure 5C**). On the other hand, only a few gene sets were enriched in the low DPT expression group, such as $CD8^+$ T cell (**Figure 5D**).

Correlation of DPT with the proportion of TICs

We analyzed the proportion of TICs subsets in PRAD samples using the CIBERSORT algorithm, constructing immune cell profiles for 21 distinct immune cell types (**Figure 6**). The results from the difference and correlation analysis revealed that a total of 6 TICs types were correlated with the expression of DPT (**Figure 7**). Among these TICs, the expression of DPT demonstrated positive correlations with 2 types of TICs, including resting mast cells and neutrophils. Conversely, 4 TICs types exhibited negative correlations with DPT expression, comprising regulatory T cells, M1 macrophages, M2 macrophages, and resting dendritic cells.

Discussion

In recent years, increasing attention has been directed toward the role of TME in PRAD progression and therapeutic resistance. As a dynamic ecosystem composed of immune cells, stromal cells, ECM, and signaling molecules, the TME not only shapes tumor behavior but

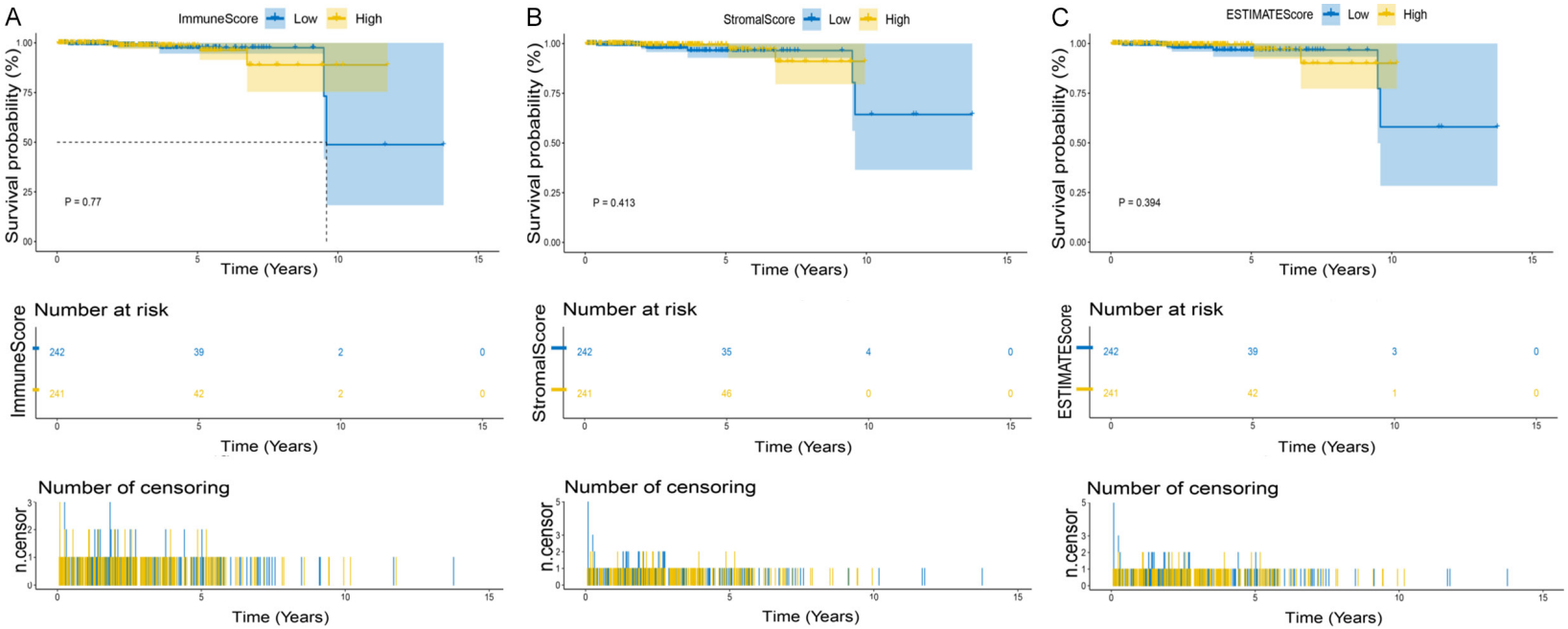

Figure 2. Correlation of scores with the survival of patients with PRAD. A. Kaplan-Meyer survival analysis for PRAD patients divided by ImmuneScore into high or low score groups (*P*=0.77, log-rank test). B. Kaplan-Meyer survival analysis for PRAD patients divided by StromalScore into high or low score groups (*P*=0.413, log-rank test). C. Kaplan-Meyer survival analysis for PRAD patients with high and low ESTIMATEScore (*P*=0.394, log-rank test).

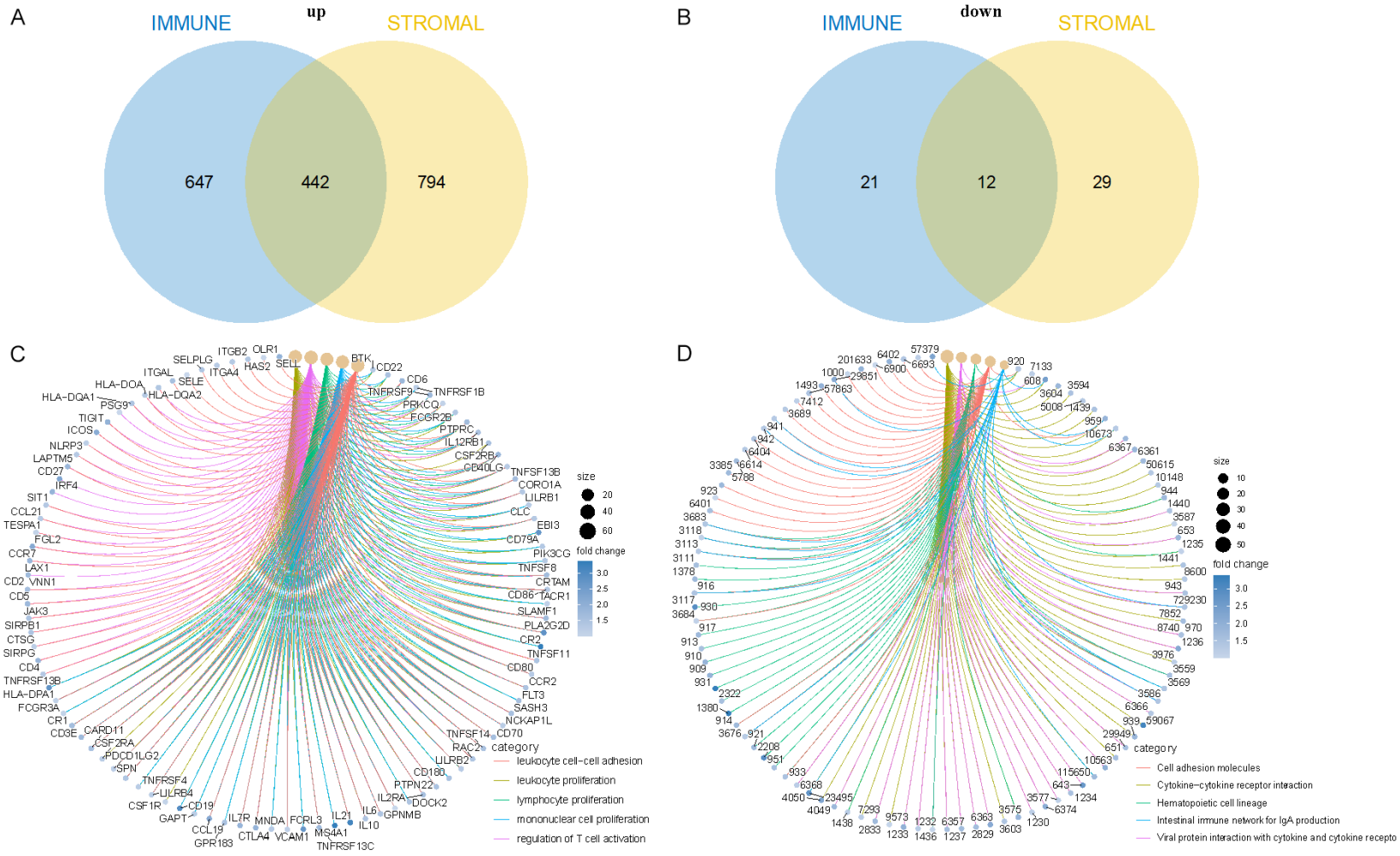

Figure 3. Screening of DEGs and enrichment analysis of GO and KEGG. A, B. Venn plots showing common up-regulated and down-regulated DEGs shared by ImmuneScore and StromalScore. C, D. GO and KEGG enrichment analysis for 455 DEGs, terms with p and q<0.05 were considered to be enriched significantly.

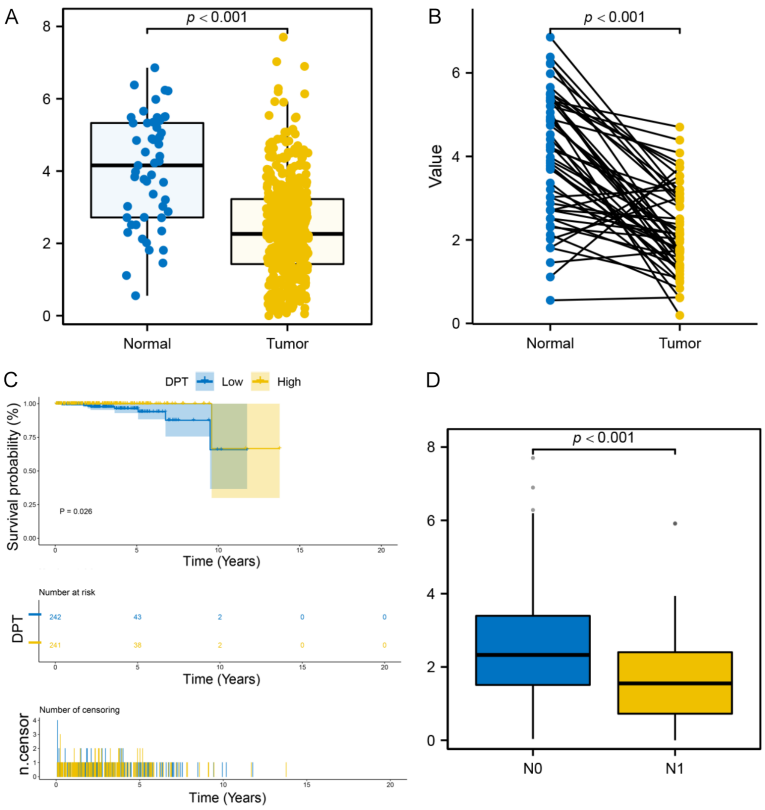

Figure 4. The differentiated expression of DPT in samples and correlation with survival and clinicopathological staging characteristics of PRAD patients. A. Differentiated expression of DPT in the normal and tumor samples. B. Paired differentiation analysis for expression of DPT in the normal and tumor samples deriving from the same one patient. C. Survival analysis for PRAD patients with high and low DPT expression (*P*=0.026, log-rank test). D. The correlation of DPT expression with clinicopathological staging characteristics.

also influences treatment outcomes, particularly in the context of immunotherapy.

TME plays a crucial role in the progression of tumors. The influence of TME extends to the metabolic reprogramming of cancer cells. The interaction between cancer cells and stromal fibroblasts can enhance the expression of metabolic enzymes, promoting a glycolytic switch that supports tumor growth [27]. The regulatory T cells (Tregs) in TME help tumor survival and progression through IL-2/IL-2 receptor-dependent and CTLA-4-dependent mechanisms [28]. However, the immunological characteristics of TME in PRAD remain incompletely understood, and effective immune biomarkers are still lacking. In this study, we identified DPT as a TME-associated molecule with potential prognostic value and regulatory relevance in PRAD.

Our results demonstrated that DPT expression is significantly decreased in tumor tissues compared to normal prostate tissues, and its low expression was associated with shorter overall survival. These findings suggest that DPT may function as a tumor suppressor in prostate cancer. Importantly, GSEA analysis revealed that high DPT expression was positively correlated with immune-related signaling pathways, including allograft rejection, complement activation, and apical junction pathways - implying that DPT may contribute to an immunologically active TME. In contrast, low DPT expression was associated with proliferative and metabolic pathways such as E2F targets and G2M checkpoint signaling, indicating a potential shift toward immune escape and tumor aggressiveness. These findings suggest that DPT may play a tumor suppressive role in PRAD through immune regulation of TME. From a mechanistic perspective, DPT is known to participate in ECM organization and cell adhesion, potentially influencing immune cell trafficking and spatial architecture within TME. Previous studies in melanoma, hepatocellular carcinoma, and breast cancer have indicated that DPT may regulate macrophage polarization, inhibit tumor growth, and modulate drug resistance through ECM-immune cell interactions [16, 17, 29-31].

Immune cell infiltration is a critical prognostic factor in solid tumors, including PRAD. The presence and activity of different TICs can significantly influence tumor behavior, disease progression, and response to therapy. Our study demonstrates that high levels of DPT expression are significantly associated with several positively correlated TICs, including dormant mast cells and neutrophils. However, its mechanism of the immune infiltration of patients with PRAD is still unclear. Studies have shown mast cells play a complex role in tumor immunity, promoting local immune responses and potentially improving TME [32]. In PRAD,

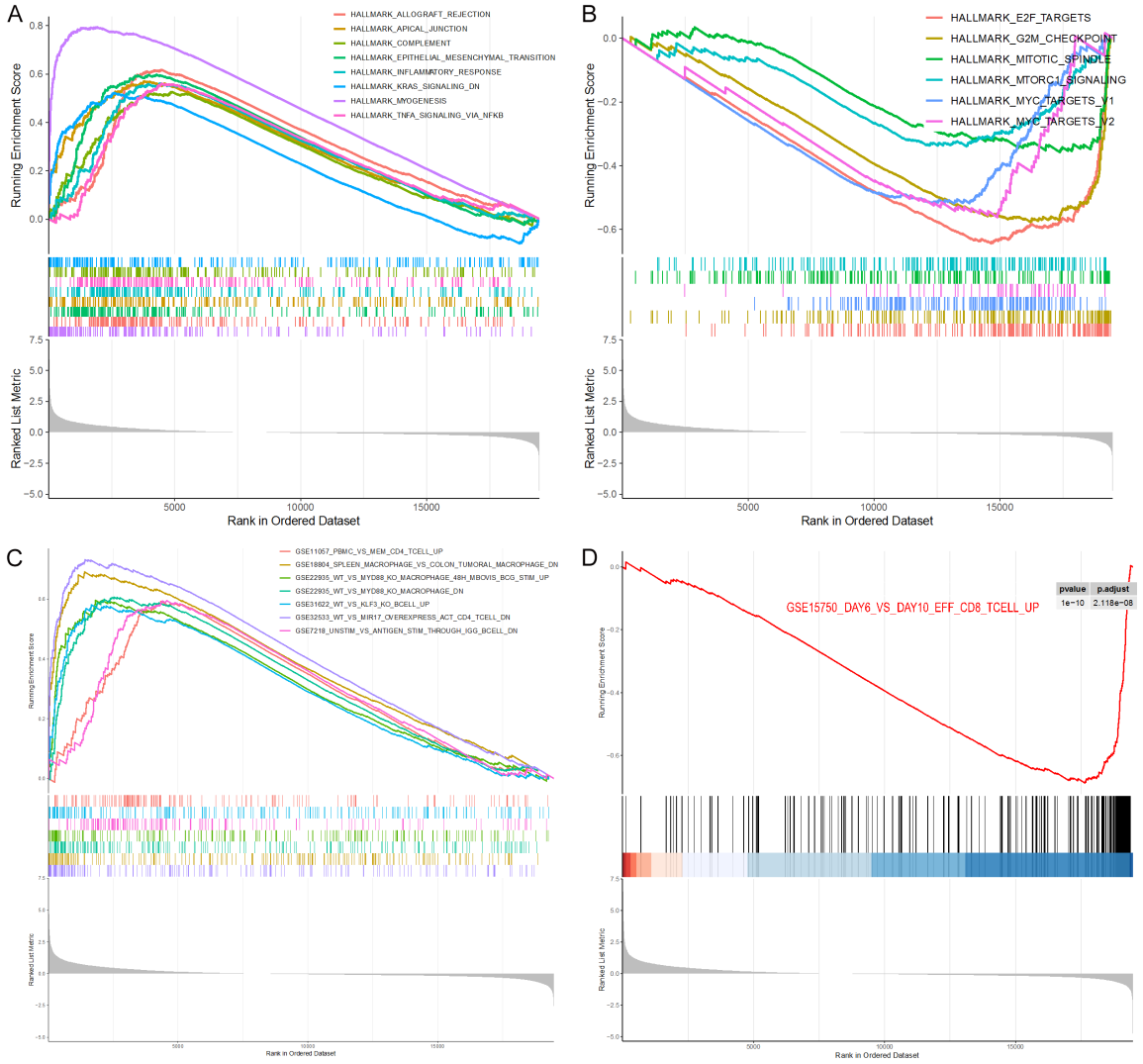

Figure 5. GSEA for samples with high DPT expression and low expression. A. The enriched gene sets in HALLMARK collection by the high DPT expression PRAD sample. Each line representing one particular gene set with unique color. Only gene sets with NOM $P<0.05$ and FDR $q<0.06$ were considered significant. B. Enriched gene sets in HALLMARK by PRAD samples with low DPT expression. C. Enriched immunologic gene sets in C7 collection by high DPT expression PRAD patients. D. Enriched gene sets in C7 collection by the low DPT expression PRAD patients.

the presence of dormant mast cells may correlate with enhanced immune surveillance, contributing to better overall survival [33]. Neutrophils are also believed to have protective roles in tumor immunity by activating T cells through the release of reactive oxygen species and cytokines [34]. Therefore, the positive correlation between high DPT levels and these TICs likely reflects a favorable immune environment that enhances patient survival. Conversely, our findings reveal significant associations between DPT expression and various negatively correlated TICs, including Tregs, M1 and M2 macrophages, and dormant dendritic cells. While Tregs are essential for maintaining immune tolerance, their increased presence often correlates with the suppression of effective anti-tumor immune responses, leading to disease progression [35, 36]. Typically, high levels of Tregs infiltration in tumors are associated with immune evasion and poorer clinical outcomes [37]. Although M1 macrophages are usually associated with anti-tumor immunity, the negative correlation of DPT in PRAD may indicate that higher DPT levels help inhibit M1 polarization, thus avoiding a detrimental imbalance in anti-tumor immune responses [38]. Additionally, M2 macrophages are known for

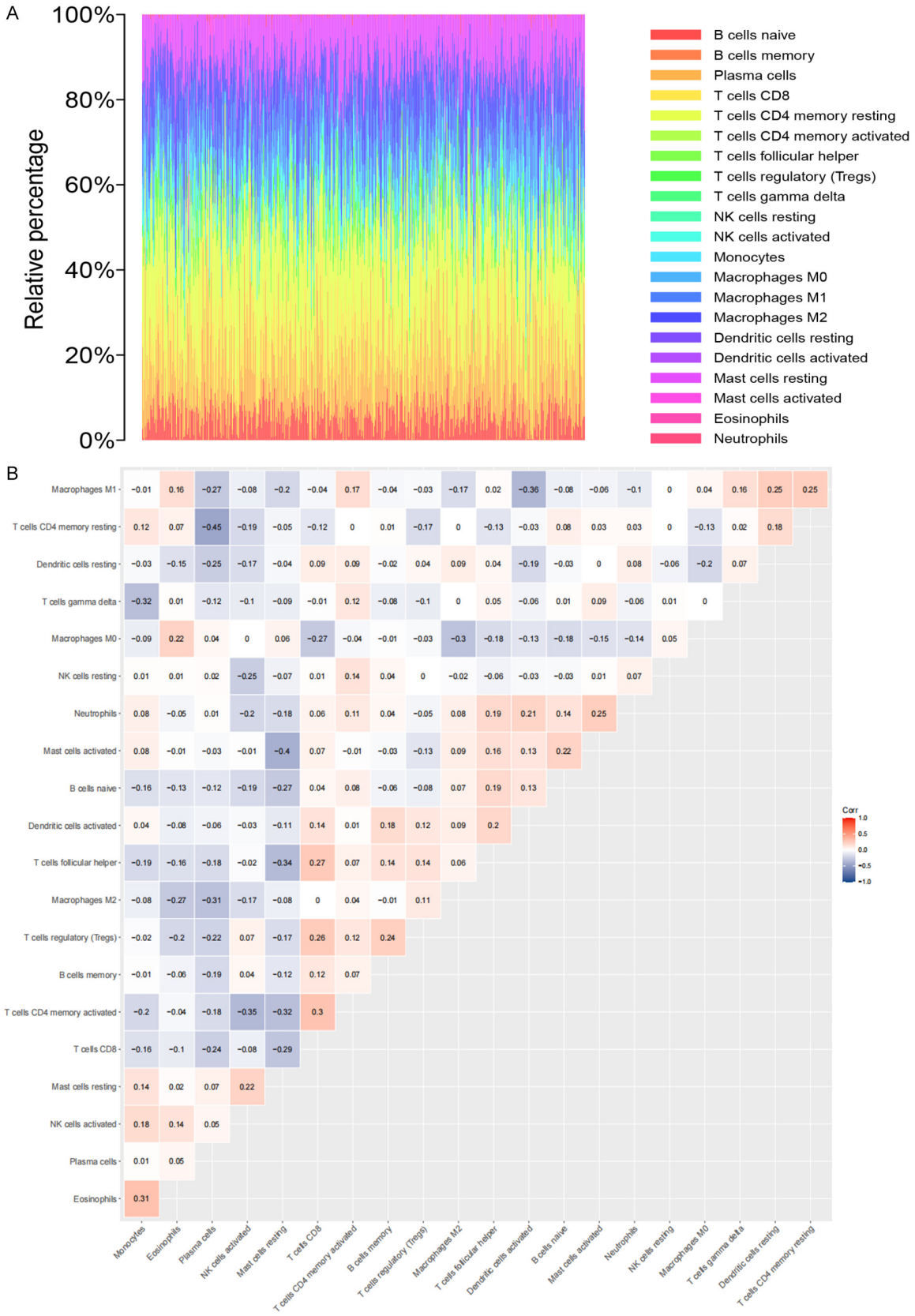

Figure 6. TICs profile in PRAD samples and correlation analysis. A. Barplot showing the proportion of TICs in PRAD samples. Column names of plot were sample ID. B. Heatmap showing the correlation between 21 kinds of TICs and numeric in each tiny box indicating the *p* value of correlation between two kinds of cells.

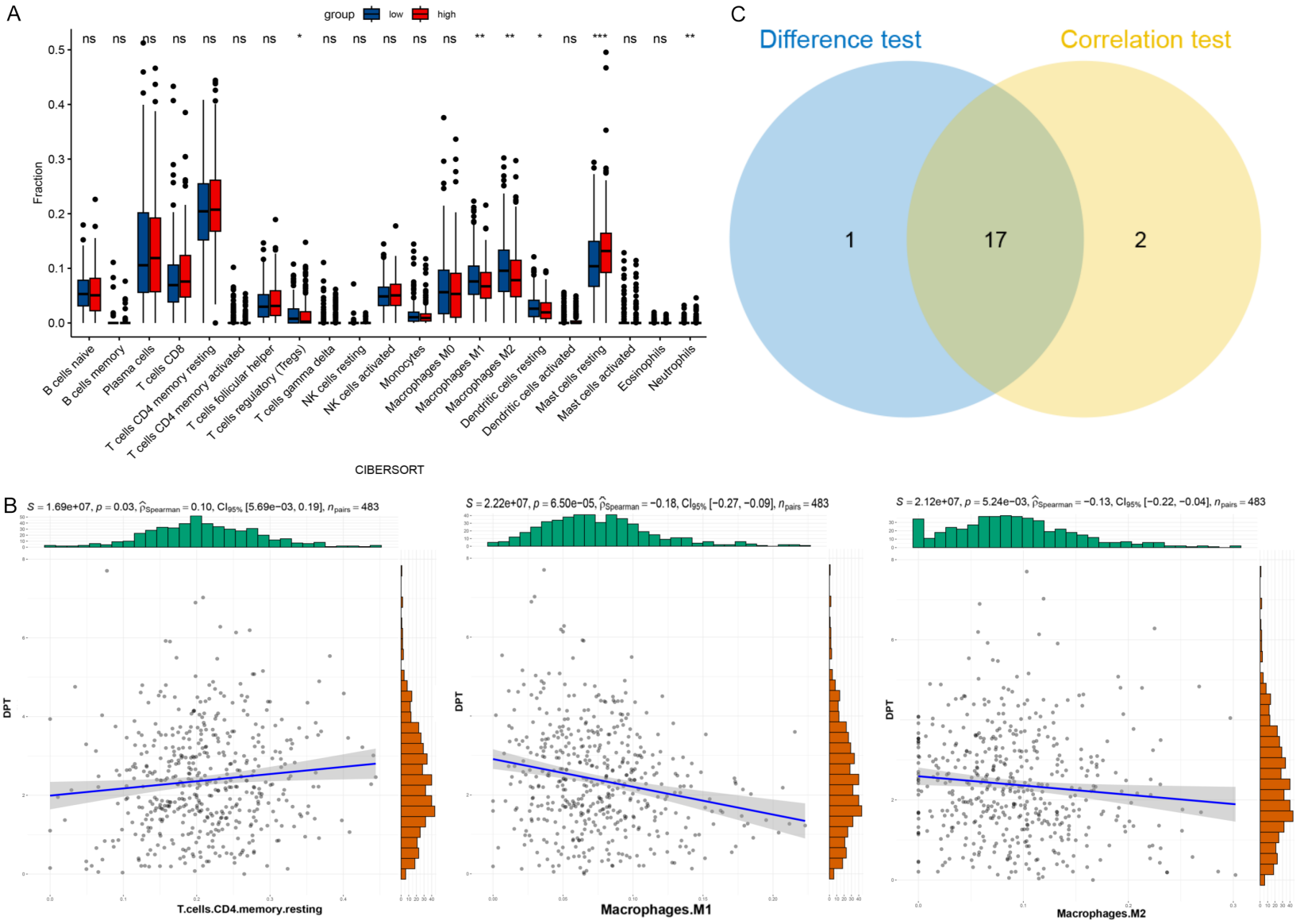
A
group low high
ns ns ns ns ns ns ns * ns ns ns ns ns ** ** * ns *** ns ns **
Fraction
0.0 0.1 0.2 0.3 0.4 0.5
B cells naive
B cells memory
Plasma cells
T cells CD8
T cells CD4 memory resting
T cells CD4 memory activated
T cells follicular helper
T cells regulatory (Tregs)
T cells gamma delta
NK cells resting
NK cells activated
Monocytes
Macrophages M0
Macrophages M1
Macrophages M2
Dendritic cells resting
Dendritic cells activated
Mast cells resting
Mast cells activated
Eosinophils
Neutrophils
CIBERSORT
C
Difference test
Correlation test
1
17
2
B
S = 1.69e+07, p = 0.03, ρ̂Spearman = 0.10, CI95% [5.69e−03, 0.19], npairs = 483
DPT
T.cells.CD4.memory.resting
S = 2.22e+07, p = 6.50e−05, ρ̂Spearman = −0.18, CI95% [−0.27, −0.09], npairs = 483
DPT
Macrophages.M1
S = 2.12e+07, p = 5.24e−03, ρ̂Spearman = −0.13, CI95% [−0.22, −0.04], npairs = 483
DPT
Macrophages.M2

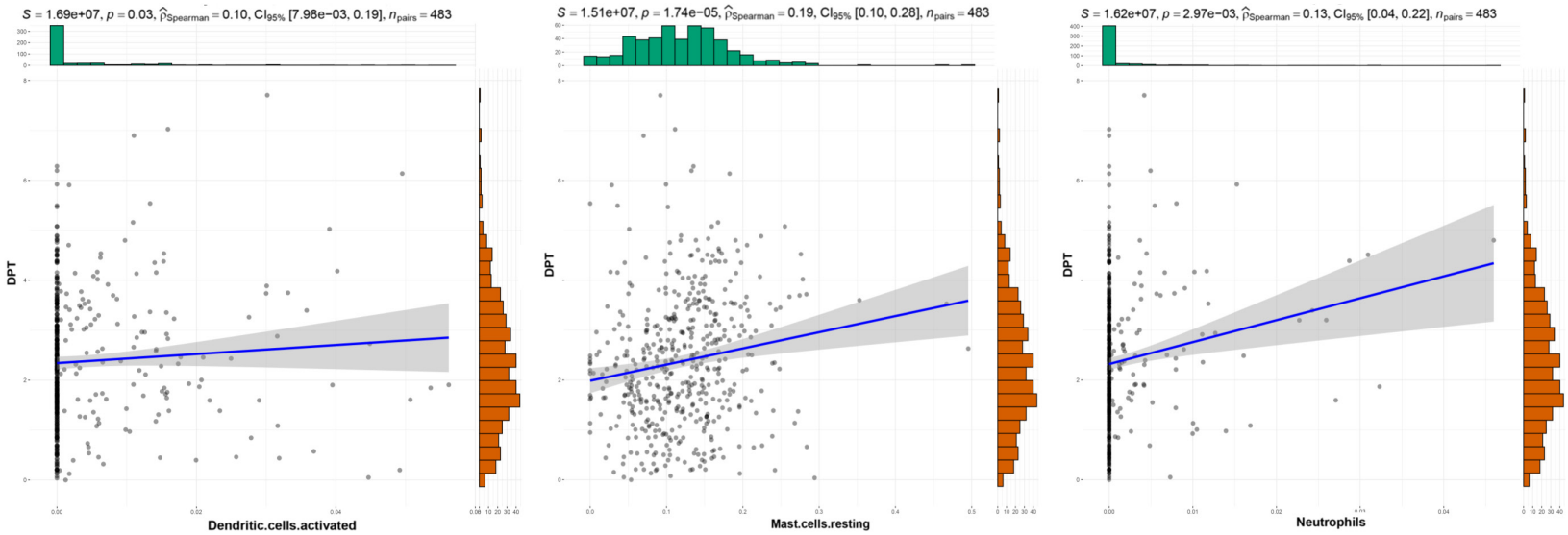

Figure 7. Correlation of TICs proportion with DPT expression. A. Violin plot showed the ratio differences of 21 kinds of immune cells between PRAD samples with low or high DPT expression, and Wilcoxon rank sum was used for the significance test. B. Scatter plot showed the correlation of 6 kinds of TICs proportion with the DPT expression (P<0.001), and Pearson coefficient was used for the correlation test. C. Venn plot displayed 17 kinds of TICs correlated with DPT expression codetermined by difference and correlation tests displayed in violin and scatter plots, respectively.

promoting tumor progression [39]. Thus, the negative correlation between DPT and M2 macrophage infiltration may suggest that elevated DPT levels reduce M2 activity, promoting a more favorable tumor prognosis [40]. The decrease in dormant dendritic cells, which are crucial for T cell activation, alongside increased DPT levels, may indicate a shift toward a lower immunogenic environment [41]. Therefore, the inverse relationship between DPT and immunosuppressive cell types further supports its role in maintaining a favorable immune microenvironment.

Nevertheless, this study is not without limitations. First, all analyses were conducted based on bulk RNA-seq data from TCGA, which may obscure spatial and cellular heterogeneity within TME. Second, the findings remain correlative in nature, and functional validation - such as knockdown or overexpression experiments in vitro and in vivo - is required to confirm the mechanistic roles of DPT in modulating immune cell infiltration and tumor progression. Third, the cohort lacked detailed treatment records, limiting our ability to assess the predictive value of DPT for therapeutic response.

In conclusion, our findings highlight DPT as a potential prognostic biomarker and immunomodulator in PRAD. By influencing immune cell infiltration and reshaping TME, DPT may offer new avenues for stratifying patients and designing immunotherapy strategies. Future studies incorporating single-cell analysis, spatial transcriptomics, and experimental validation will be essential to fully delineate the functional role of DPT and translate these findings into clinical practice.

Acknowledgements

We thank all the families for participating in this research project. This work was supported by Science Foundation of Jiangsu Province Grant BK20240371; National Science Foundation of China Grants 81901632, and the Jiangsu Province College Students' Innovation and Entrepreneurship Training Program Project (202410285273Y).

Disclosure of conflict of interest

None.

Address correspondence to: Yuting Liang, Center for Clinical Laboratory, The First Affiliated Hospital of Soochow University, Suzhou 215006, Jiangsu, China. E-mail: liangyuting666@126.com

References

[1] Sung H, Ferlay J, Siegel RL, Laversanne M, Soerjomataram I, Jemal A and Bray F. Global cancer statistics 2020: GLOBOCAN estimates of incidence and mortality worldwide for 36 cancers in 185 countries. CA Cancer J Clin 2021; 71: 209-249.

[2] Bergengren O, Pekala KR, Matsoukas K, Fainberg J, Mungovan SF, Bratt O, Bray F, Brawley O, Luckenbaugh AN, Mucci L, Morgan TM and Carlsson SV. 2022 update on prostate cancer epidemiology and risk factors-a systematic review. Eur Urol 2023; 84: 191-206.

[3] Siegel RL, Miller KD and Jemal A. Cancer statistics, 2020. CA Cancer J Clin 2020; 70: 7-30.

[4] Li G, Huang Q, Wai Wong VK, Wang W and Leung CH. Development of a dual targeting scaffold of SET7/MLL inhibitor for castration-resistant prostate cancer treatment. Genes Dis 2023; 10: 2260-2262.

[5] Kang J, La Manna F, Bonollo F, Sampson N, Alberts IL, Mingels C, Afshar-Oromieh A, Thalmann GN and Karkampouna S. Tumor microenvironment mechanisms and bone metastatic disease progression of prostate cancer. Cancer Lett 2022; 530: 156-169.

[6] Ribeiro Franco PI, Rodrigues AP, de Menezes LB and Pacheco Miguel M. Tumor microenvironment components: allies of cancer progression. Pathol Res Pract 2020; 216: 152729.

[7] Wei R, Liu S, Zhang S, Min L and Zhu S. Cellular and extracellular components in tumor microenvironment and their application in early diagnosis of cancers. Anal Cell Pathol (Amst) 2020; 2020: 6283796.

[8] Mao X, Xu J, Wang W, Liang C, Hua J, Liu J, Zhang B, Meng Q, Yu X and Shi S. Crosstalk between cancer-associated fibroblasts and immune cells in the tumor microenvironment: new findings and future perspectives. Mol Cancer 2021; 20: 131.

[9] Guo Q, Zhou Y, Xie T, Yuan Y, Li H, Shi W, Zheng L, Li X and Zhang W. Tumor microenvironment of cancer stem cells: perspectives on cancer stem cell targeting. Genes Dis 2023; 11: 101043.

[10] Dai J, Lu Y, Roca H, Keller JM, Zhang J, McCauley LK and Keller ET. Immune mediators in the tumor microenvironment of prostate cancer. Chin J Cancer 2017; 36: 29.

[11] Jansen CS, Prokhnevska N and Kissick HT. The requirement for immune infiltration and organization in the tumor microenvironment for successful immunotherapy in prostate cancer. Urol Oncol 2019; 37: 543-555.

[12] Liu CM, Hsieh CL, Shen CN, Lin CC, Shigemura K and Sung SY. Exosomes from the tumor microenvironment as reciprocal regulators that enhance prostate cancer progression. Int J Urol 2016; 23: 734-744.
[13] Chen L, Wang Y, Hu Q, Liu Y, Qi X, Tang Z, Hu H, Lin N, Zeng S and Yu L. Unveiling tumor immune evasion mechanisms: abnormal expression of transporters on immune cells in the tumor microenvironment. Front Immunol 2023; 14: 1225948.
[14] Lei X, Lei Y, Li JK, Du WX, Li RG, Yang J, Li J, Li F and Tan HB. Immune cells within the tumor microenvironment: biological functions and roles in cancer immunotherapy. Cancer Lett 2020; 470: 126-133.
[15] Chu GC, Chung LWK, Gururajan M, Hsieh CL, Josson S, Nandana S, Sung SY, Wang R, Wu JB and Zhau HE. Regulatory signaling network in the tumor microenvironment of prostate cancer bone and visceral organ metastases and the development of novel therapeutics. Asian J Urol 2019; 6: 65-81.
[16] Ye D, Wang Y, Deng X, Zhou X, Liu D, Zhou B, Zheng W, Wang X and Fang L. DNMT3a-dermatopontin axis suppresses breast cancer malignancy via inactivating YAP. Cell Death Dis 2023; 14: 106.
[17] Liu S, Qiu J, He G, Geng C, He W, Liu C, Cai D, Pan H and Tian Q. Dermatopontin inhibits WNT signaling pathway via CXXC finger protein 4 in hepatocellular carcinoma. J Cancer 2020; 11: 6288-6298.
[18] Lu Y, Lin Y, Zhang X, Yan J, Kong Z, Zhang L, Wang C, Huang Y, Zhao S and Li Y. LncRNA-AP006284.1 promotes prostate cancer cell growth and motility by forming RNA-DNA triplexes and recruiting GNL3/SFPQ complex to facilitate RASSF7 transcription. Genes Dis 2022; 10: 317-320.
[19] Jin J, Zhang Y, Cao J, Feng J, Liang Y, Qiao L, Feng B, Tang Q, Qiu J and Qian Z. PYGO2 as a novel prognostic biomarker and its correlation with immune infiltrates in liver cancer. Am J Clin Exp Immunol 2025; 14: 23-33.
[20] Zhang Y, Zhou T, Tang Q, Feng B and Liang Y. Identification of glycosyltransferase-related genes signature and integrative analyses in patients with ovarian cancer. Am J Clin Exp Immunol 2024; 13: 12-25.
[21] Lin K, Wang T, Tang Q, Chen T, Lin M, Jin J, Cao J, Zhang S, Xing Y, Qiao L and Liang Y. IL18R1-related molecules as biomarkers for asthma severity and prognostic markers for idiopathic pulmonary fibrosis. J Proteome Res 2023; 22: 3320-3331.
[22] Zhou T, Cao J, Tang Q, Jin J, Liang Y and Feng B. Exploring the role of NAA40 in immune infiltrates and prognostic prediction in hepatocellular carcinoma. Am J Clin Exp Immunol 2024; 13: 26-34.
[23] Feng B, Zhang Y, Qiao L, Tang Q, Zhang Z, Zhang S, Qiu J, Zhou X, Huang C and Liang Y. Evaluating the significance of ECSCR in the diagnosis of ulcerative colitis and drug efficacy assessment. Front Immunol 2024; 15: 1426875.
[24] Zhou T, Zhang Y, Cao J, Tang Q, Liang Y, Zhang S, Hu M, Feng B and Jin J. Identification of immune infiltration-related ZNF480 for predicting prognosis in breast cancer. Am J Clin Exp Immunol 2025; 14: 1-13.
[25] Feng B, Zhou T, Guo Z, Jin J, Zhang S, Qiu J, Cao J, Li J, Peng X, Wang J, Xing Y, Ji R, Qiao L and Liang Y. Comprehensive analysis of immune-related genes for classification and immune microenvironment of asthma. Am J Transl Res 2023; 15: 1052-1062.
[26] Zhang Y, Feng B, Liang Y, Tang Q, Zhang S, Zhang Z, Xu L and Yin J. Prognostic significance of LRPPRC and its association with immune infiltration in liver hepatocellular carcinoma. Am J Clin Exp Immunol 2024; 13: 105-116.
[27] Mori JO, Elhussin I, Brennen WN, Graham MK, Lotan TL, Yates CC, De Marzo AM, Denmeade SR, Yegnasubramanian S, Nelson WG, Denis GV, Platz EA, Meeker AK and Heaphy CM. Prognostic and therapeutic potential of senescent stromal fibroblasts in prostate cancer. Nat Rev Urol 2024; 21: 258-273.
[28] Karpisheh V, Mousavi SM, Naghavi Sheykholeslami P, Fathi M, Mohammadpour Saray M, Aghebati-Maleki L, Jafari R, Majidi Zolbanin N and Jadidi-Niaragh F. The role of regulatory T cells in the pathogenesis and treatment of prostate cancer. Life Sci 2021; 284: 119132.
[29] Xu P, Li S, Liu K, Fan R, Liu F, Zhang H, Liu D and Shen D. Downregulation of dermatopontin in cholangiocarcinoma cells suppresses CCL19 secretion of macrophages and immune infiltration. J Cancer Res Clin Oncol 2024; 150: 66.
[30] Yuan Z, Li Y, Zhang S, Wang X, Dou H, Yu X, Zhang Z, Yang S and Xiao M. Extracellular matrix remodeling in tumor progression and immune escape: from mechanisms to treatments. Mol Cancer 2023; 22: 48.
[31] Welinder C, Jönsson G, Ingvar C, Lundgren L, Baldetorp B, Olsson H, Breslin T, Rezeli M, Jansson B, Laurell T, Fehniger TE, Wieslander E, Pawlowski K and Marko-Varga G. Feasibility study on measuring selected proteins in malignant melanoma tissue by SRM quantification. J Proteome Res 2014; 13: 1315-1326.
[32] Aponte-López A and Muñoz-Cruz S. Mast cells in the tumor microenvironment. Adv Exp Med Biol 2020; 1273: 159-173.

[33] Guo X, Sun M, Yang P, Meng X and Liu R. Role of mast cells activation in the tumor immune microenvironment and immunotherapy of cancers. Eur J Pharmacol 2023; 960: 176103.
[34] Shafqat A, Khan JA, Alkachem AY, Sabur H, Alkattan K, Yaqinuddin A and Sing GK. How neutrophils shape the immune response: reassessing their multifaceted role in health and disease. Int J Mol Sci 2023; 24: 17583.
[35] Tanaka A and Sakaguchi S. Regulatory T cells in cancer immunotherapy. Cell Res 2017; 27: 109-118.
[36] Li Y, Zhang C, Jiang A, Lin A, Liu Z, Cheng X, Wang W, Cheng Q, Zhang J, Wei T and Luo P. Potential anti-tumor effects of regulatory T cells in the tumor microenvironment: a review. J Transl Med 2024; 22: 293.
[37] Yano H, Andrews LP, Workman CJ and Vignali DAA. Intratumoral regulatory T cells: markers, subsets and their impact on anti-tumor immunity. Immunology 2019; 157: 232-247.
[38] Shapouri-Moghaddam A, Mohammadian S, Vazini H, Taghadosi M, Esmaeili SA, Mardani F, Seifi B, Mohammadi A, Afshari JT and Sahebkar A. Macrophage plasticity, polarization, and function in health and disease. J Cell Physiol 2018; 233: 6425-6440.
[39] Feng D, Shi X, Li D, Wu R, Wang J, Wei W and Han P. M2 macrophage-related molecular subtypes and prognostic index for prostate cancer patients through integrating single-cell and bulk RNA sequencing analysis. Genes Dis 2024; 11: 101086.
[40] Chen Y, Zhang S, Wang Q and Zhang X. Tumor-recruited M2 macrophages promote gastric and breast cancer metastasis via M2 macrophage-secreted CHI3L1 protein. J Hematol Oncol 2017; 10: 36.
[41] Gardner A and Ruffell B. Dendritic cells and cancer immunity. Trends Immunol 2016; 37: 855-865.